Kerr Electro-optic Field Measurement and Charge Dynamics in Transformer-oil/Solid Composite Insulation Systems

H. Okubo, R. Shimizu, A. Sawada, K. Kato, N. Hayakawa

Nagoya University, Nagoya, Japan

and M. Hikita

Kyushu Insitute of Technology, Japan

ABSTRACT

We measured the electric field in transformer oil/solid composite insulation system under dc voltage application using a Kerr electro-optic measurement system. When a pressboard was inserted at the center between two parallel-plane electrodes, the electric field at the mid-point between the pressboard and the cathode decreased with time. On the other hand, the electric field at the mid-point between the pressboard and the anode increased initially with time, reached a maximum value and then fell down. We measured also the electric field before and after polarity reversal of the dc voltage. The results revealed that the electric field after polarity reversal reached a magnitude 2.7× as much as the average dc applied field. We interpreted the above results on the time transition of the electric field in terms of a charge dynamic model, considering the difference in charge accumulation speed on the pressboard between positive and negative charges. This model was verified to be applicable to the time transition of the electric field in oil/solid composite system and BTA added oil/solid composite system as well.

1. INTRODUCTION

FOR long-distance electric power transmission, high voltage dc (HVDC) power transmission is advantageous [1–2]. In dc converter transformers, dielectric liquids such as transformer oil are used generally, with solid insulating materials such as paper and pressboard. Under dc voltage application, the liquid moves and gradually charges are accumulated on the surface of the solid materials. Therefore, the electric field distribution in liquid/solid composite dc insulation systems cannot be calculated easily. Moreover, in dc converter transformers, polarity reversal of dc voltage would be one of the most important factors to be considered for dc insulation design. From the above background, it follows that it is very important to measure directly an electric field distribution in such a composite insulation system. Such measurements allow us to get both fundamental understanding of the charge dynamics and guidelines for the insulation design of the apparatus under dc voltage application.

The Kerr electro-optic field measuring technique made it possible to obtain electric field distribution in liquid dielectrics. Kerr electro-optic effect relies on the birefringence of liquid that is induced when an electric field is applied. Hence, this technique allows us to measure the electric field with no disturbance. In recent years, extensive research on the direct field measurement in liquids have appeared using the Kerr effect [3–9].

This paper describes measurement results of the time transition of the electric field in transformer oil/solid composite insulation system for dc voltage application using the Kerr electro-optic technique. We also measure the electric field distribution under polarity reversal of dc voltage and discuss the charge dynamics in the composite insulation system.

2. EXPERIMENTAL SYSTEM

Figure 1 illustrates the experimental setup for measurement of the electric field in transformer oil using the Kerr effect. The Kerr constant of transformer oil is so small, $B \sim 3 \times 10^{-15}$ m/V^2 that we used a combined technique of ac electric field modulation and circularly polarized light to enhance the measuring sensitivity [4]. A pair of electrodes made of brass with 100 mm in length l and 65 mm in width, and gap length $g = 10$ mm were placed in parallel each other in a stainless steel test cell filled with transformer oil. A dc voltage $V_{dc} =$

1070–9878/97/$3.00

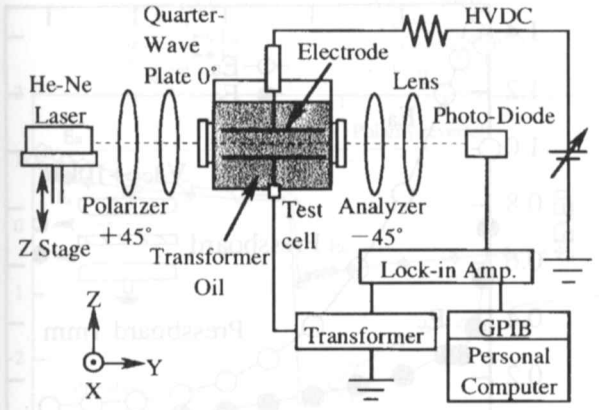

Figure 1. Experimental setup.

+10 or −10 kV was applied to the HV electrode, and at the same time, a 1 kHz ac voltage $V_{ac} = 200V_{peak}$ was superimposed on the grounded electrode.

As a light source, a He-Ne laser (7.0 mW, 632.8 nm) was used. The laser beam passes through a polarizer and a quarter-wave plate to get circular polarization. After passing a test cell and an analyzer, the laser beam was detected with a photodiode. The detected signal was taken to a lock-in amplifier synchronized at the modulation frequency. For the arrangement of the optical system shown in Figure 1, the electric field strength E from the light intensity is calculated as follows [9]

$$\frac{I_{1\omega}}{I_{dc}} = 2\pi \frac{E_{dc}E_{ac}}{E_{max}^2} \tag{1}$$

where E_{dc} and E_{ac} are the applied dc field and the superimposed ac field, and $I_{1\omega}$ and I_{dc} are the first harmonic component and the dc component of the light intensity, respectively. E_{max} is the electric field strength when the light intensity is at maximum, and is defined as

$$E_{max} = \frac{1}{\sqrt{2Bl}} \tag{2}$$

We measured the field in oil with two transformer oil/pressboard (PB) composite systems with gap length 10 mm; (1) the grounded electrode was covered with 1 mm thick pressboard and (2) 1 mm thick PB was inserted in the gap between the two electrodes. To discuss the charge dynamics in oil, we also measured the electric field in the oil when the PB was replaced with 1 mm thick polymethyl methacrylate (PMMA). On the other hand, we investigated the temporal development of the electric field in the oil under polarity reversal of dc voltage. After $V_{dc} = +10$ kV was applied to the HV electrode for several hours in case (2), the polarity reversal was made; *i.e.* the HV electrode was grounded, and then $V_{dc} = -10$ kV was applied.

The oil was degassed and then dry nitrogen gas was filled in the cell. All measurements were performed at room temperature with atmospheric pressure.

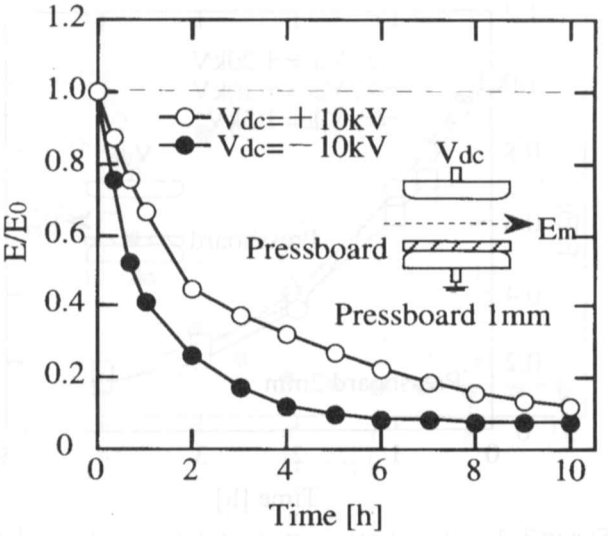

Figure 2. Time dependence of normalized electric field E_m in oil with pressboard on the grounded electrode for +10 kV and −10 kV dc voltages.

3. EXPERIMENTAL RESULTS

3.1. ELECTRIC FIELD IN OIL WITH SOLID DIELECTRICS COVERING THE GROUNDED ELECTRODE

Figure 2 shows the time dependence of the electric field E_m at the center of the oil gap for a parallel-plane electrode configuration with 1 mm thick PB on the grounded electrode. In Figure 2, the vertical axis scale shows the electric field normalized by the electric field E_0 just after V_{dc} application. It is seen in this Figure that the electric field E_m in oil for $V_{dc} = -10$ kV decreases more rapidly with time than that for $V_{dc} = +10$ kV. The reason for the reduction of the electric field is that the charges having the same polarity as the applied dc voltage accumulate on PB and relax the electric field in the oil. Thus, the experimental results suggest that negative charges in oil accumulate on the PB surface faster than positive charges.

Figure 3 displays the time dependence of the electric field E_m with 2 mm thick PB on the grounded electrode for $V_{dc} = +5$, +10 and +20 kV. In Figure 3, the vertical axis shows the electric field normalized by the electric field E_0 immediately after V_{dc} application. As can be seen, the time dependence of the normalized electric field for different V_{dc} falls along a similar curve. The results indicate that the time evolution of E_m/E_0 is independent of the applied dc voltage.

To discuss the influence of solid dielectric material on the time transition of the electric field in oil, we replaced PB with 1 mm thick PMMA. Figure 4 shows the time dependence of electric field E_m in oil with 1 mm thick PMMA. As seen in Figure 4, the plot of E_m *vs.* time is independent of the polarity of V_{dc}; this result differs from that for oil/PB composite system given in Figure 2. The discussion for these results will be given later in Section 4.

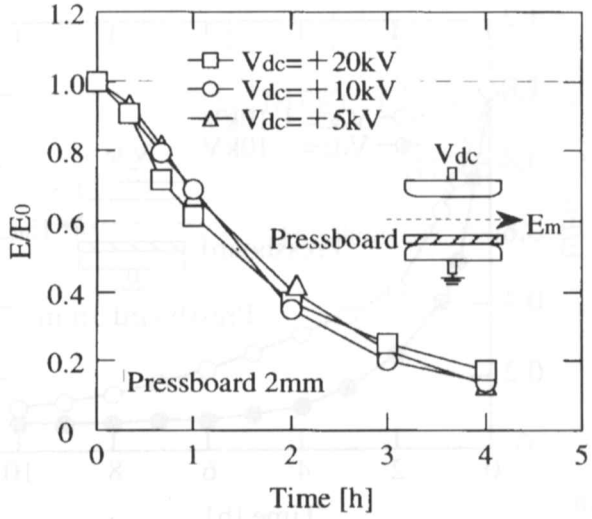

Figure 3. Time dependence of normalized electric field E_m in oil with pressboard on the grounded electrode for different dc voltages.

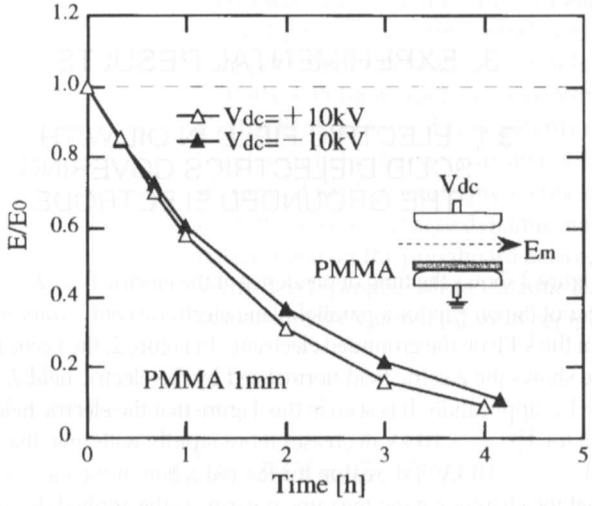

Figure 4. Time dependence of normalized electric field E_m in oil with PMMA on the grounded electrode for +10 kV and −10 kV dc voltages.

3.2. ELECTRIC FIELD IN OIL WITH SOLID DIELECTRICS INSERTED BETWEEN TWO ELECTRODES

Figure 5 displays the time dependence of electric fields E_a and E_c in oil with 1 mm thick PB inserted at the center between two electrodes for $V_{dc} = +10$ kV. Here, E_a denotes the electric field at the mid-point between the PB and the anode, and E_c denotes that between the PB and the cathode. As can be seen in this Figure, E_c decreases with time and becomes nearly constant at 0.6 kV/cm. On the other hand, E_a initially increases with time, reaches a peak of $\sim 1.4\times$ as much as the average field E_0 at 10 min, then decreases and becomes nearly constant. Another experiments revealed that similar time evolutions of the electric field in oil appeared for different dc applied voltages: $V_{dc} = +5$, +20 and −10 kV. The anode side field E_a shows a peak, and the cathode side E_c reduces monotonically. The time t_p elapsed from voltage application to the peak of E_a

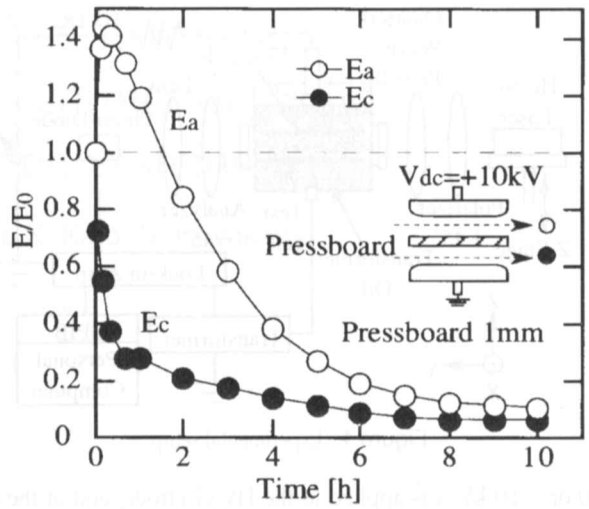

Figure 5. Time dependence of normalized electric fields E_a and E_c in oil with pressboard inserted at the center between two electrodes.

proved to be almost constant at 10 to 20 min for all V_{dc}.

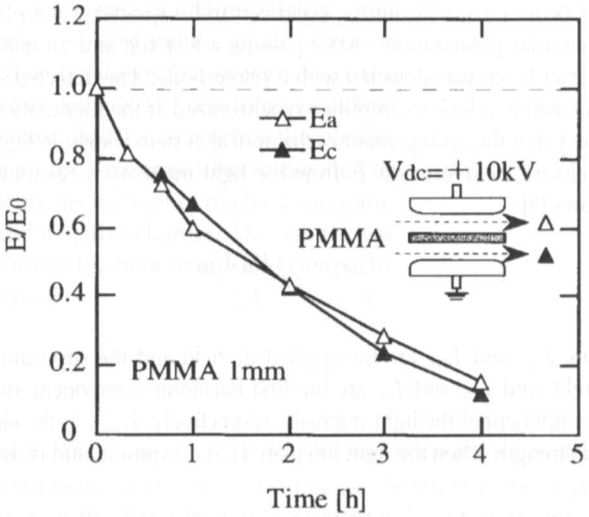

Figure 6. Time dependence of normalized electric fields E_a and E_c in oil with PMMA inserted at the center between two electrodes.

The result for oil/PMMA is displayed in Figure 6 for $V_{dc} = +10$ kV. As seen in Figure 6, both E_a and E_c decrease with increasing time. These time transitions of E_a and E_c in Figure 6 are the same trend as those of E_m in Figure 4. We will discuss these results in Section 4.

3.3. ELECTRIC FIELD AT THE POLARITY REVERSAL OF DC VOLTAGE

Figure 7 shows the time dependence of electric fields E_a and E_c in oil with 1 mm thick PB inserted at the center of two electrodes when the polarity of dc voltage was reversed after 5 h after initiation of voltage ($t_r = 5$ h). As can be seen, $|E_a|$ is much larger than $|E_c|$ after the polarity reversal. It is also seen that $|E_c|$ decreases with time, while $|E_a|$ increases with time, reaches a peak at 10 min after polarity reversal and then decreases. Moreover, it should be noticed

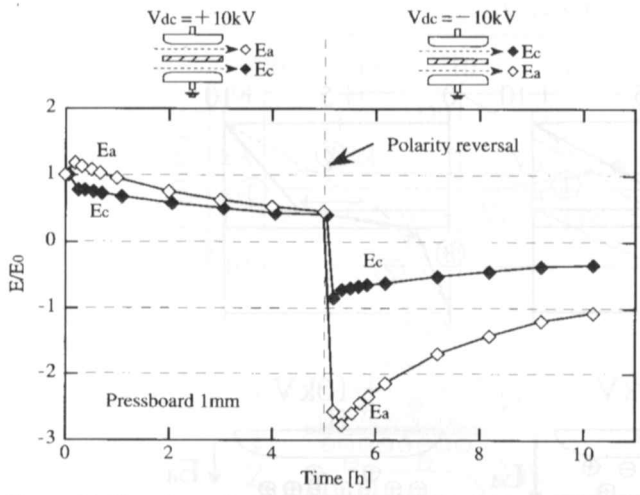

Figure 7. Time dependence of normalized electric fields E_a and E_c in oil with pressboard inserted at the center between two electrodes before and after polarity reversal of dc voltage.

that the maximum peak value of $|E_a|$ reaches the magnitude 2.4× as much as the average field E_0.

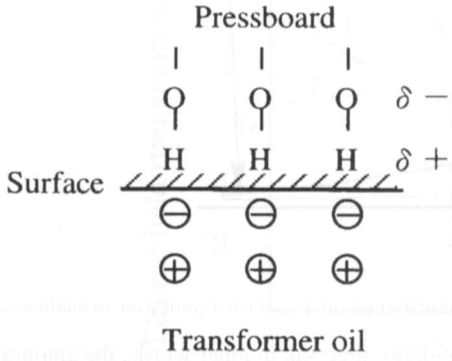

Figure 8. Concept of surface of pressboard.

4. DISCUSSION

4.1. POLARITY DEPENDENCE OF ELECTRIC FIELD *vs.* TIME

As seen in Figure 2, the time evolution of electric field E_m in oil with PB on the electrode depended upon the polarity of dc applied voltage. The reason for the polarity difference can be considered as follows: it is well known that insulating paper and PB tend to adsorb negative charge in transformer oil [10], so that negative charges are more likely to accumulate on PB than positive charges as can be seen in Figure 8. Thus, E_m for $V_{dc} = -10$ kV decreases more rapidly with time than that for $V_{dc} = +10$ kV in oil/PB as seen in Figure 2.

On the other hand, since PMMA has no charge-adsorbing property, the charge accumulation speed in oil/PMMA is unchanged with respect to the polarity of dc applied voltage, resulting in no polarity difference of E_m as seen in Figure 4.

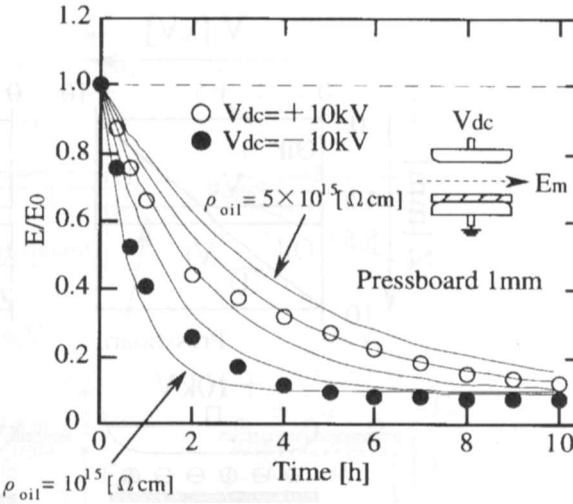

Figure 9. Time dependence of normalized electric field in oil calculated by equivalent circuit for transformer oil/pressboard composite insulation system ($\rho_{oil}/\rho_{PB} = 1/100$).

4.2. TIME CONSTANT OF ELECTRIC FIELD *vs.* TIME

Next, we discuss the time constant of the time transition of electric field E_m in oil. For a composite system, E_m immediately after voltage application is determined by the permittivity division of voltage, whereas E_m at the steady state dc voltage application is determined by the resistivity ratio. Figure 9 displays calculated E_m in oil with 1 mm thick PB on the grounded electrode when the composite system is assumed to be expressed by CR equivalent circuit. In addition, the resistivity ratio of oil to PB is assumed as $\rho_{oil}/\rho_{PB} = 1/100$. As can be seen in Figure 9, no proper curves can be fitted to the experimental data but they lie around the curve with $\rho_{oil} \fallingdotseq 10^{15}$ [Ωcm]. The discrepancy may arise from liquid movement, nonlinear electric field dependence of the pressboard resistivity, and so on [11].

4.3. CHARGE DYNAMICS IN OIL/SOLID DIELECTRICS COMPOSITE SYSTEM

As seen in Figure 5, E_a *vs.* time characteristics are different from those of E_c *vs.* time; only E_a has a peak value when the PB was inserted at the center between two electrodes. To explain these results, we propose a model of charge dynamics in oil/PB composite system as illustrated in Figure 10. Before voltage application, one can assume that no charge accumulates on PB, and the same number of negative and positive charges exist in oil. Then, $V_{dc} = +10$ kV is applied to the HV electrode.

At the instant of voltage application, the voltage distributes depending on the permittivity ratio of oil and PB, as shown in Figure 10(a). Since negative charges accumulate on PB faster than positive ones as mentioned above, the potential V_l of the lower surface of the PB decreases rapidly at $t = t_p$ as seen in Figure 10(b). It is also assumed that the electric field built in PB remains unchanged within the short period while V_l changes; the assumption is reasonable because the resistivity of PB is much larger than that of oil. In this case,

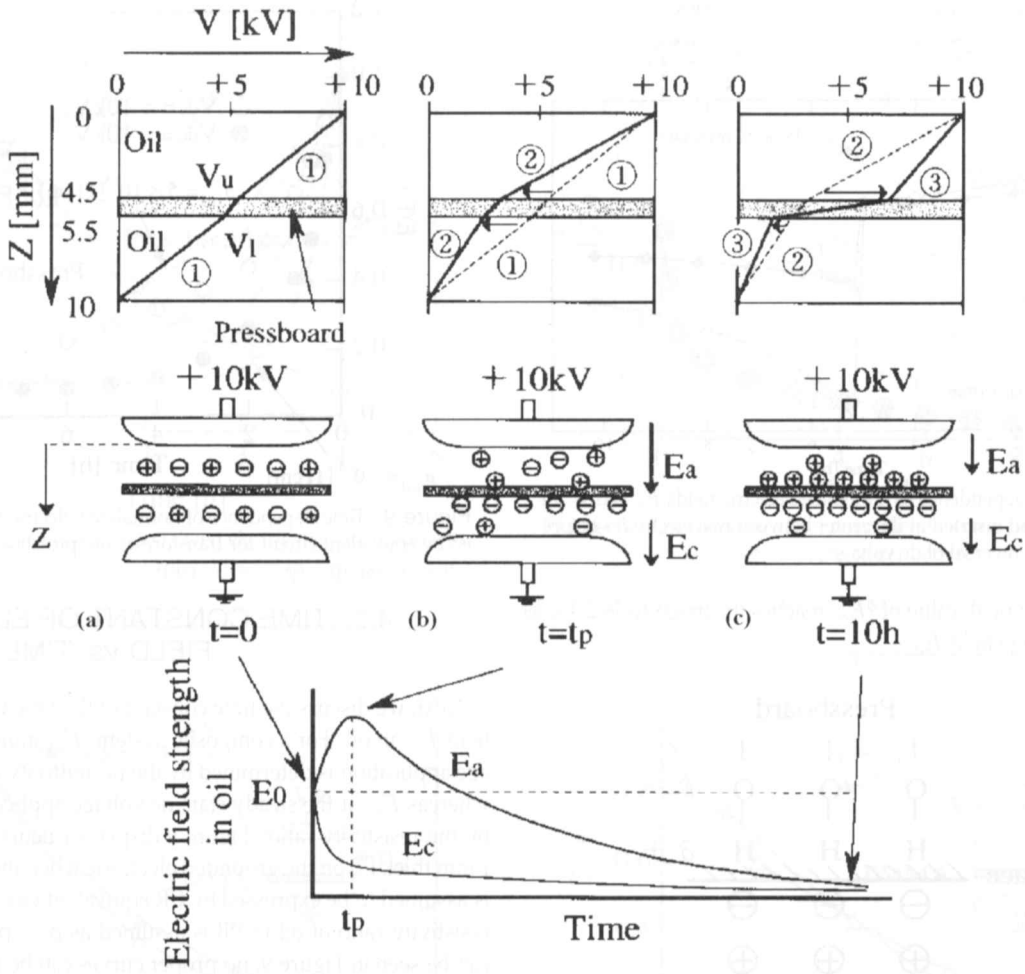

Figure 10. Schematic illustration of potential distribution and charge dynamics of transformer oil/pressboard composite insulation system.

the potential V_u of the upper surface of the PB also decreases with V_l. It follows that E_a starts increasing with time at first and then has a peak value. Since positive charges gradually accumulate on PB and V_u begins to increase with time, E_a decreases as seen in Figure 10(c) after $t = t_p$.

On the other hand, as described before, the accumulation speed of positive and negative charges are the same in oil/PMMA composite system from Figure 4. Accordingly, the consideration is consistent with the observed time transition of E_a and E_c given in Figure 6.

4.4. CHARGE DYNAMICS AFTER POLARITY REVERSAL

Next, we try to explain the time dependence of the electric field after the polarity reversal of V_{dc} shown in Figure 7, using the above charge dynamic model. Before the polarity reversal at the time t_r, positive and negative charges are considered to accumulate on PB surface as depicted in Figure 11(a). After polarity reversal of V_{dc} under those conditions, $|E_a|$ at $t = t_r$ is larger than $|E_0|$ because of the accumulated charges on PB as seen in Figure 11(b). If the polarity of V_{dc} were reversed at the steady-state, both $|E_a|$ and $|E_c|$ in oil could be twice of $|E_0|$. The reason why $|E_a|$ was larger than $|E_c|$ immediately after $t = t_r$ in Figure 7 is that $|E_c|$ was smaller than $|E_a|$ before the polarity reversal; in other words, the amount of negative charges accumulated on the PB may exceed that of positive ones. The phenomenon that $|E_a|$ has a peak value after the polarity reversal can also be explained, as seen in Figure 11(c), in terms of the same processes as those discussed in Figure 10. Accordingly, the proposed charge dynamic model allows the estimation of $|E_a| > 2|E_0|$ at polarity reversal. That is, peak field $|E_a|$ after the polarity reversal is higher than the initial peak field after dc voltage application because of the accumulated charges on the PB.

Figure 12 shows the obtained maximum electric field strength immediately after polarity reversal as a function of polarity reversal time t_r. In this Figure, the vertical axis represents the electric field normalized by $|E_0|$, and the mark $\star$ (white star) denotes the maximum peak value of $|E_a|$ at $t = t_r + t'_p$. In Figure 12, we can find the maximum value of $|E_a|$ at $t = t_r + t'_p$ reaches the magnitude 2.7× as much as $|E_0|$. It is pointed out from the above experimental results that the polarity reversal of dc voltage is one of the most important factors for the insulation design of dc power apparatus and then for determination of a testing voltage of the apparatus.

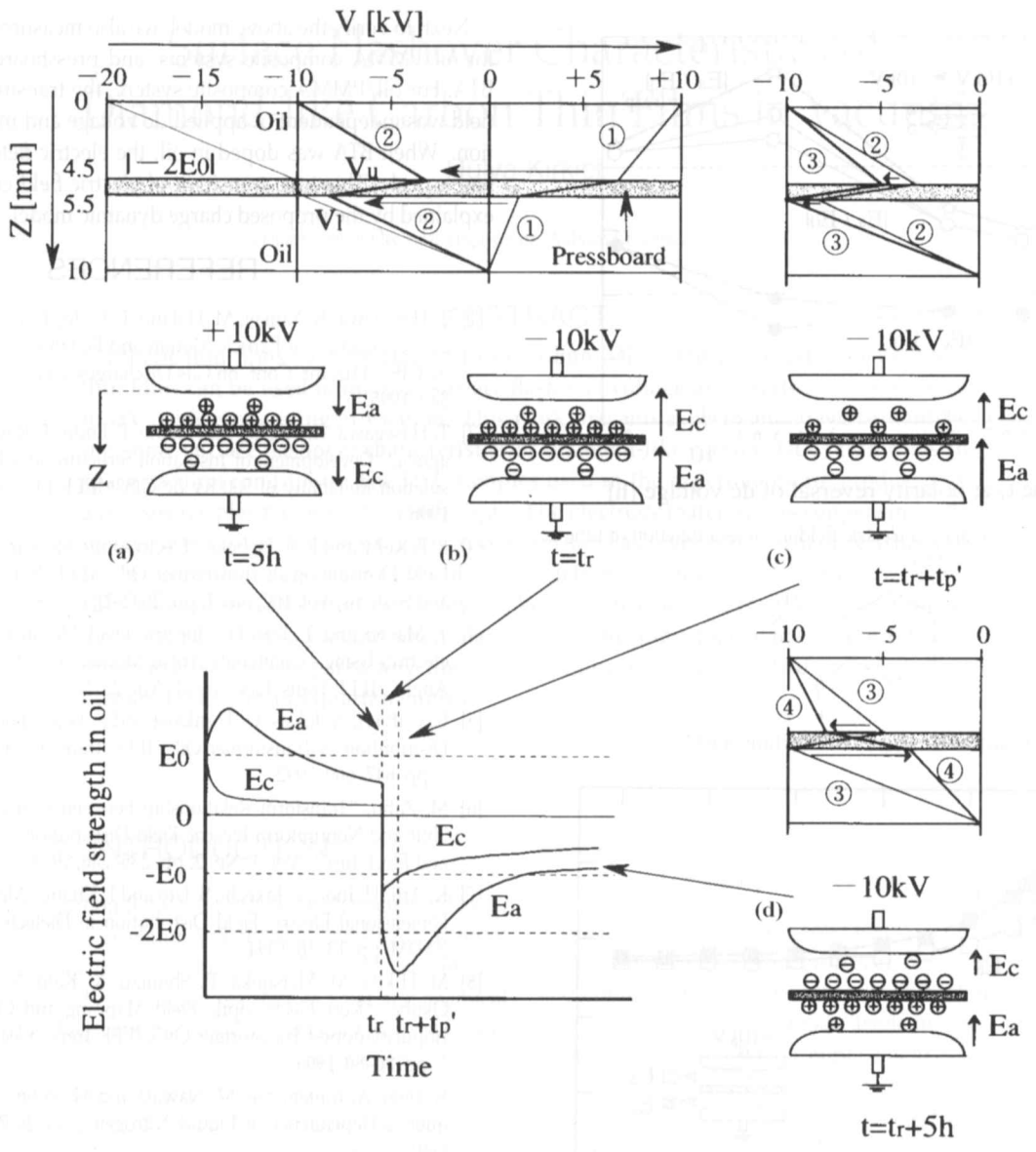

Figure 11. Schematic illustration of potential distribution and charge dynamics of transformer oil/pressboard composite insulation system after polarity reversal.

4.5. ELECTRIC FIELD IN OIL ADDED WITH BTA

BTA (1,2,3-benzotriazol) is known as an antistatic agent for streaming electrification [10]. BTA has chemical structure as shown in Figure 13 and is easily adsorbed to the insulating paper and PB, and draws positive charge in transformer oil. Thus, the proposed charge dynamic model is expected to permit E_c instead of E_a has a peak value in oil doped with BTA.

Figure 14 depicts measured time transition of the electric fields E_a and E_c in oil added with BTA of 10 ppm for oil/PB composite system. As can be seen in this Figure, in BTA-doped oil, E_a decreases with time, while E_c initially increases with time, reaching a peak and then decreases. These time dependencies of E_a and E_c are completely opposite to those for fresh oil/PB composite system as shown in Figure 5. The results for BTA doped oil/PB are interpreted in terms of the higher accumulation speed of positive charges on PB surface than that of negative ones which are brought about by the BTA additive. Thus, the proposed charge dynamic model was verified experimentally.

5. CONCLUSIONS

We measured directly the electric field by the Kerr electro-optic method in transformer oil/solid dielectrics composite insulation system under dc voltage application and discussed the charge dynamics in oil. When a pressboard was inserted at the center between two parallel-plane electrodes, the electric field E_a at the anode side proved to have a peak 1.4× as much as the average field E_0. The results of E_a *vs.* time characteristics were explained well by the charge dynamic model based on the negative charge-dominant property of pressboard. Moreover, experimental results revealed that after

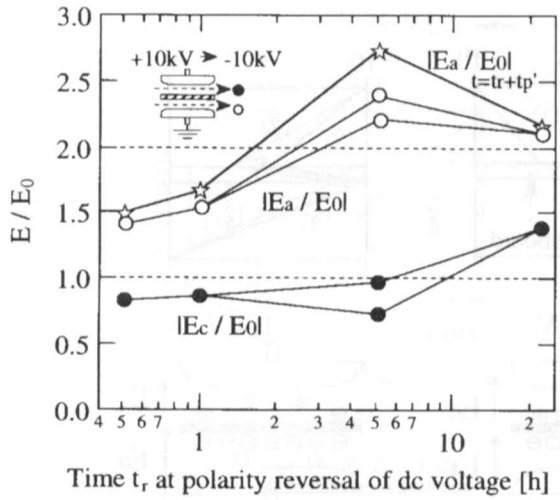

Figure 12. Enhancement of electric field in oil as a function of time at polarity reversal of dc voltage.

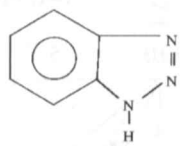

Figure 13. Molecular structure of BTA.

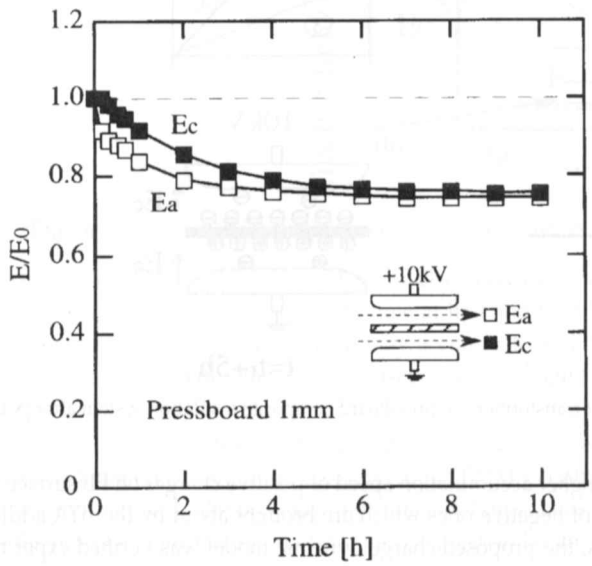

Figure 14. Time dependence of normalized electric fields E_a and E_c in oil added with BTA of 10 ppm. Pressboard is inserted at the center between two electrodes.

polarity reversal of dc voltage the electric field strength $|E_a|$ reached the magnitude $\sim 2.7\times$ as much as $|E_0|$.

Next, to verify the above model, we also measured the electric field for oil/PMMA composite systems, and pressboard/oil added with BTA. For oil/PMMA composite system, the transition of the electric field was independent of applied dc voltage and measurement position. When BTA was doped in oil, the electric field at cathode side had a peak. This time transition of electric field could also be well explained by the proposed charge dynamic model.

REFERENCES

[1] T. Hasegawa, K. Yamaji, M. Hatano, F. Endo, T. Rokunohe and T. Yamagiwa, "Control of Particle Motion and Reliability Improvement in HV dc GIS", 11th Int. Conf. on Gas Discharges and their Appli., pp. I-346–349, 1995.

[2] T. Hasegawa, K. Yamaji, M. Hatano, F. Endo, T. Rokunohe and T. Yamagiwa, "Development of Insulation Structure and Enhancement of Insulation Reliability of 500 Kv dc GIS", IEEE PES 96 SM 395-4 PWRD, 1996.

[3] E. F. Kelly and R. E. Hebner, "Electro-optic Measurement of the Electric Field Distribution in Transformer Oil", IEEE Trans. Power Apparatus and Systems, Vol. 102, No. 7, pp. 2092–2097, 1983.

[4] T. Maeno and T. Takada, "Electric Field Measurement in Liquid Dielectrics Using a Combination of ac Modulation and a Small Retardation Angle", IEEE Trans. Elect. Insul., Vol. 22, No. 4, pp. 503–508, 1987.

[5] U. Gäfvert, A. Jaksts, C. Törnkvist and L. Walfridsson, "Electrical Field Distribution in Transformer Oil", IEEE Trans. Elect. Insul., Vol. 27, No. 3, pp. 647–660, 1992.

[6] M. Zahn, "Transform Relationship between Kerr-effect Optical Phase Shift and Nonuniform Electric Field Distribution", IEEE Trans. Dielect. and Elect. Insul., Vol. 1, No. 2, pp. 235–246, 1994.

[7] K. Arii, H. Ihori, I. Takechi, S. Uto and I. Kitani, "Measurement of Three Dimensional Electric Field Distribution in Dielectric Liquids", 4th ICPADM, pp. 13–16, 1994.

[8] M. Hikita, M. Matsuoka, R. Shimizu, K. Kato, N. Hayakawa and H. Okubo, "Kerr Electro-optic Field Mapping and Charge Dynamics in Impurity-doped Transformer Oil", IEEE Trans. Elect. Insul., Vol. 3, No. 1, pp. 80–86, 1996.

[9] K. Imai, A. Kanematsu, M. Nawata and M. Zahn, "Kerr Constant Frequency Dependence in Liquid Nitrogen", 3rd ICPADM, pp. 280–283, 1991.

[10] M. Ieda, K. Goto, H. Okubo, T. Miyamoto, H. Tsukioka and Y. Kohno, "Suppression of Static Electrification of Insulated Oil for Large Power Transformers", IEEE Trans. Elect. Insul., Vol. 23, No. 1, pp. 153–157, 1988.

[11] I. Ohshima, Y. Maikawa, T. Hamano, O. Sakakura and M. Honda, "HVDC Field Characteristics with and without ac Superposed in Converter Transformer", 3rd ISH, 11. 18, 1979.

Manuscript was received on 23 July 1996, in revised form 2 January 1997.